Congestion Resiliency for Data-Partitioned H.264/AVC Video Streaming over IEEE 802.11e Wireless Networks

***Ismail Ali, Sandro Moiron, Martin Fleury and Mohammed Ghanbari**
University of Essex, Colchester CO4 3SQ, United Kingdom

ABSTRACT

This paper considers the impact of data partitioning form on wireless network access control and proposes a selective dropping scheme based on dropping the partition carrying intra-coded macroblocks. Data partitioning is an error resiliency technique that allows unequal error protection for transmission over 'lossy' channels. Including a per-picture, cyclic intra-refresh macroblock line guards against temporal error propagation. The paper shows that, by this scheme, when congestion occurs, it is possible to gain up to 2 dB in video quality over assigning a stream to a single IEEE 802.11e access category. The scheme is shown to be consistently advantageous in indoor and outdoor wireless scenarios over other ways of assigning the partitioned data packets to different access categories. This counter-intuitive scheme for access control purposes reverses the priority usually given to partition-B data packets over that of partition-C.

Keywords: H.264/AVC, Data Partitioning, Intra-Refresh, IEEE 802.11e, Congestion Control.

INTRODUCTION

Advances in source coding continue to encourage the growth of video streaming services. Thus, as the H.264/AVC (Advanced Video Coding) encoder can achieve up to 50% increase in compression ratio (Wiegand et al., 2003) compared to an MPEG-2 encoder, it is particularly appropriate for bandwidth-limited WLANs, which is why H.264/AVC has already been adopted for 3GPP's Multimedia Broadcast Multicast Service (Afzal et al., 2006).

As part of its network-friendly approach (Liu et al., 2005), H.264/AVC introduced a set of error resilience tools (Stockhammer et al., 2003) to improve robustness to packet loss in transmission over error-prone networks. Among those tools were data partitioning and distributed intra-refresh macroblocks (MBs). Data partitioning is a way of separating out data from a compressed bit-stream according to its importance in reconstructing a video stream. H.264/AVC Network Abstraction Layer units (NALUs) are per-slice containers for packet transmission. Data partitioning splits video content into three partitions: Data Partition A (DP-A), B (DP-B) and C (DP-C) (Wenger, 2003) of decreasing importance for decoder reconstruction purposes. This partitioning scheme allows the more important data to be given preferential treatment.

To protect the stream against temporal error propagation, it is becoming common to distribute intra-refresh MBs across the video pictures (Schreier & Rothermel, 2006) rather than provide periodic intra-coded frames (I-frames), as periodic refresh I-frames cause a sudden increase in the data rate. As a consequence, DP-B will become enlarged as it is this partition that contains the major portion of data from intra coded MBs. With or without an enlarged DP-B, protecting DP-A, -B, and -C in an unequal error protection scheme seems sensible. For example, in Barma et al. (2005) a combination of hierarchical modulation and forward error protection was applied.

In this paper, we show that when cyclic intra-refresh lines are applied then DP-B packets become a better candidate to drop at network access time than DP-C packets. Thus, in our scheme, DP-C packets are given greater protection than DP-B packets. To illustrate the proposed dropping scheme for data-partitioned, cyclic intra-refresh provisioned video streaming, we applied the IEEE 802.11e (IEEE, 2005) for priority-controlled access to a WLAN.

In Ksentini et al. (2006), the authors proposed a cross-layer architecture to improve H.264/AVC video delivery over IEEE 802.11e. Each partition of the compressed bit-stream was mapped to a different IEEE 802.11e access category (AC), allowing the prioritization of packets bearing the more important DP-A and DP-B data. However, their scheme was aimed at transmission issues, especially reduction of end-to-end delay and minimization of packet loss rate, rather than congestion during access to the network. Furthermore, unlike our scheme DP-B data is favored for protection over protection of DP-C.

In Bernardini et al. (2007), another protection scheme was compared to wireless transmission with multiple description coding (MDC). If DP-A data is well protected then partitioned data transmission results in over 10 dB improvement in quality over an MDC scheme but otherwise MDC is preferable. However, again that paper's primary concern was transmission issues. Similarly, in Haywood et al. (2009) measurements indicated that using a single IEEE 802.11e AC was preferable over splitting the H.264 data-partitioned video packets across the IEEE 802.11e ACs. However, in their experiments DP-B and DP-C packets were assigned to the same IEEE 802.11e AC. Periodic Instantaneous Decoding Refresh (IDR)-pictures were used and given the same high priority as DP-A packets.

In Cranley et al, (2007), the TXOPLimit parameter that in part governs the relative access to other ACs was varied for the IEEE 802.11e designated video AC. It was found that the TXOP parameter could be dynamically varied when video packet bursts arrived. However, if video was given too much privilege then this could disadvantage voice traffic. Varying that parameter also requires modification of the configuration at all wireless stations. A preliminary conference version of this current paper (Ali et al., 2010) has been expanded to improve the presentation of data-partitioning and intra-refresh MBs in the methodology Section. Extensive tests also have verified the operation of the proposed scheme for a range of settings and channel propagation models.

This paper's contribution is a congestion-resilient scheme for data-partitioned video streams protected by intra-refresh MB lines. (An intra-refresh MB line is a row of intra-refresh MBs.) In these circumstances, DP-B is generally larger than would otherwise be the case. However, the

data in DP-B that potentially helps to mitigate channel errors, intra-coded MBs, are given lower priority at network access time in the proposed scheme. Because the area occupied by the intra refresh line corresponds to a comparatively limited part of a video frame, the impact of dropping packets formed from DP-B (mostly containing intra refresh line data) is reduced. The paper supplies generalized confirmation of this counter-intuitive dropping policy as well as an IEEE 802.11e case study.

The remainder of this paper is organized as follows: The next Section introduces data partitioning and intra refresh line error resilience techniques. The impact of introducing an intra-refresh line on the relative size of DP-B is also analyzed and then a practical implementation of the proposed scheme is presented. The paper then presents the framework used to assess the video quality under uniform and network drop conditions. The following Section goes on to present results for a random packet drop model, where drops occur according to a uniform distribution, and a generalized multi-hop wireless network congestion scenario. Finally, some concluding remarks are made and the future development of the proposed scheme is outlined.

METHODOLOGY

The H.264/AVC codec conceptually separates the Video Coding Layer (VCL) from the Network Abstraction Layer (NAL). The VCL specifies the core compression features, while the NAL supports delivery over various types of networks. In a communication channel, the quality of service is affected by two parameters: bandwidth and channel errors. Therefore, adaptation to communication channels as well as video compression efficiency provided by the VCL should be carefully considered. The NAL facilitates the delivery of the H.264/AVC VCL data to the underlying transport layers such as RTP/IP, H.32X and MPEG-2 transport systems. The concept of the NAL, together with the error resilience features in H.264/AVC, allows communication over a variety of different channels. Each NAL unit (NALU) can be considered as a packet that contains a header and a payload. The 8-bit header, Figure 1, specifies the NALU payload type (*nal_unit_type*) and the relative importance of NALU (*nal_ref_idc*) while the payload contains the related data. Table 1 is a summarized list of different NALU types. NALUs 6 to 12 are non-VCL units containing additional information such as parameter sets and supplemental information. NALUs 1 to 5 contain different VCL data, as described after the introduction of the slice concept.

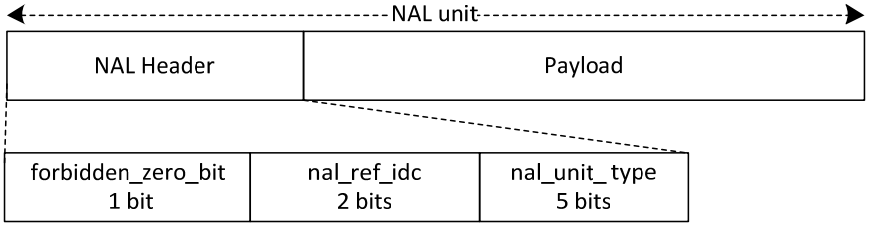

Figure 1. NAL unit format.

Table 1. NAL unit types.

NAL unit type	Class	Content of NALU
0	-	Unspecified
1	VLC	Coded slice
2	VLC	Coded slice partition A
3	VLC	Coded slice partition B
4	VLC	Coded slice partition C
5	VLC	Coded slice of an IDR picture
6-12	Non-VLC	Suppl. info., Parameter sets, etc.
13-23	-	Reserved
24-31	-	Unspecified

Each H.264/AVC picture can be divided into several slices, each of which contains a variable number of MBs. Variable Length Coding (VLC) of the compressed data takes place at the final stage of a hybrid codec. In the H.264/AVC standard, arithmetic coding replaced other forms of entropic coding in earlier codecs. In each slice, the arithmetic coder is aligned and its predictions are reset. Hence, every slice in the frame is independently decodable. Therefore, slices contain re-synchronization markers that prevent error propagation to the entire picture. Each slice is placed within a separate NALU.

The slices of an Instantaneous Decoder Refresh (IDR) picture are located in NALUs of type 5, while those belonging to P-, B-, or I-pictures are placed in NALUs of type 1. When data partition is enabled, NALUs of type 2, 3, and 4 are used to accommodate the partitioned data. In NALUs of type 1 and 5, all the data from the coded blocks are encapsulated into the packet in the order they are generated by the encoder. In Type 5, all parts of the compressed bit-stream are equally important, while in type 1, the MB addresses and motion vectors (MVs) are much more important than the (integer-valued) Discrete Cosine Transform (DCT) coefficients. In the event of errors in this type of packets, the fact that symbols appearing earlier in the bit-stream suffer less from errors than those which come later means that bringing the more important parts of the video data (such as headers and MVs) ahead of the less important data or separating the more important data altogether for better protection against errors can significantly reduce the effect of channel errors. In the standard video codecs, this is known as data partitioning.

Data Partitioning

As previously mentioned, in H.264/AVC, when data partitioning is enabled, every slice is divided into up to three separate partitions. DP-A, packed into NALUs of type 2, comprises the most important information of the compressed video bit stream from I, P, and B-pictures, including the MB addresses, motion vectors and essential headers. DP-B carries transform coefficients from intra coded (spatially predicted) MBs and is packed into NALUs of type 3. DP-C, packed into NALUs of type 4, carries transform coefficients from inter coded (temporally predicted) MBs.

Intra-coded MBs are usually applied to mitigate error propagation from temporally predicted frames. However, when an MB is intra coded, spatial prediction uses pixels from neighboring

macroblocks. If these neighbors are temporally predicted, error propagation might arise and further propagate errors into the intra-coded MB. Since intra- and inter-coded MBs are transported by different partition types, that is DP-B and DP-C respectively, an inter packet dependency is implicitly introduced. In order to avoid this dependency, constrained intra prediction (CIP) was enabled (Dhondt et al., 2007), which prevents the use of inter predicted neighbors for intra prediction.

Intra-Refresh MBs

In order to limit error propagation from temporally predicted frames, the periodic insertion of intra-refresh MB lines in a cyclic pattern within successive temporally predicted video pictures is applied. A traditional alternative way to do this is to insert periodic I-frames usually every 12 or 15 frames, that is every half-second according to frame rate. The spatially-encoded MBs of the I-frame halt the temporal error propagation and act as anchor points for a future set of frames. Unfortunately, the insertion of I-frames leads to sudden data transmission peaks due to the lower coding efficiency of spatial prediction when compared with the temporal prediction used in P and B frames. Therefore, distributed insertion of intra-refresh MBs is an alternative that should be considered.

In the JM (JVT, 2010) implementation of the H.264/AVC codec (Wiegand et al., 2003), two main methods of distributed intra insertion are available: either random placement of intra-refresh MBs within each frame; or forcing a line of intra-coded MBs within each P-frame on a cyclic basis. In the latter forced intra-refresh method, the line size can be increased to a region or slice (Tran et al., 1997) in order to control the rate that the total picture area is refreshed. Against this suggestion must be balanced the overhead from including a complete line or region of MBs, as such MBs are more costly to encode than temporally predicted blocks. Another possibility is to adaptively alter the extent of MB provision (Liang et al., 2006) according to scene content and channel conditions. This is most suitable for live encoding and is not a general method.

The objective of inserting intra-refresh MB lines (Schreier & Rothermel, 2006) is to mitigate error propagation at the cost of lower coding efficiency than purely predictive inter coding. Using a horizontal (or vertical) sliding intra-refresh line, Figure 2, reduces the error drift arising from packet loss without the instantaneous rise in the data rate when periodic I-frames are inserted. Provided a cyclic pattern of lines are transmitted, the sequence is completely refreshed after each cycle. However, it should be carefully noted that an intra-coded MB line within a temporally predicted frame represents a significant percentage of the bits devoted to compressing the whole frame. Nonetheless, a packet containing data from a line of intra-coded MBs represents a small portion of the image area. Therefore, only a small potential quality penalty arises from the loss of packets containing intra-refresh MBs due to the small image area affected. The scheme hereby described exploits this feature and proposes to selectively discard DP-B mostly containing intra-refresh MB line data in preference to dropping packets belonging to DP-C. DP-C is of course the residual information contained in the quantized DCT coefficients.

Figure 2. Cyclic intra-refresh MB line technique for the *Paris* test sequence, showing successive lines in lighter shading, with slice boundaries also shown.

Although each slice contains up to three partitions, each partition may be further split into several packets due to network packetization constraints, which impose a maximum number of bytes per packet. The result is a variable number of packets per frame, the number of which depends on the content complexity. It is advisable to configure the encoder itself to restrict the packet size so that each slice is carried by a single packet and individually decodable. This overcomes the problem arising from network-level segmentation when a single slice is split into multiple packets resulting in inter packet dependency. If any of those packets of the split slice is erroneous then the whole slice becomes non decodable. Figure 3 shows the percentage of data occupied by each partition type for a selection of well-known test videos in Common Intermediate Format (CIF) (352 × 288 pixel/picture) with a Constant Bit-Rate (CBR) target of 1 Mbps. The data from DP-C dominates, while in some sequences DP-B is hardly used.

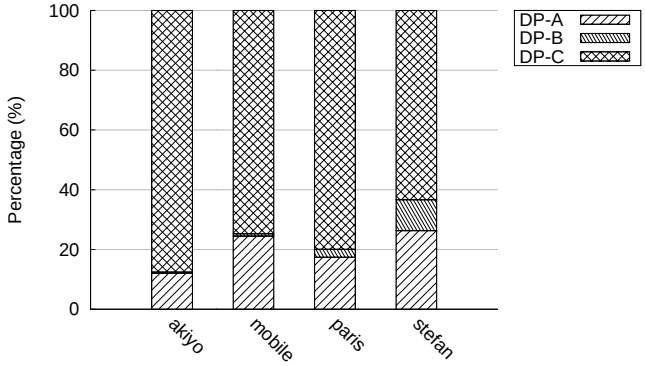

Figure 3. Percentage of data for partitions A, B and C in a variety of sequences without an intra-refresh line.

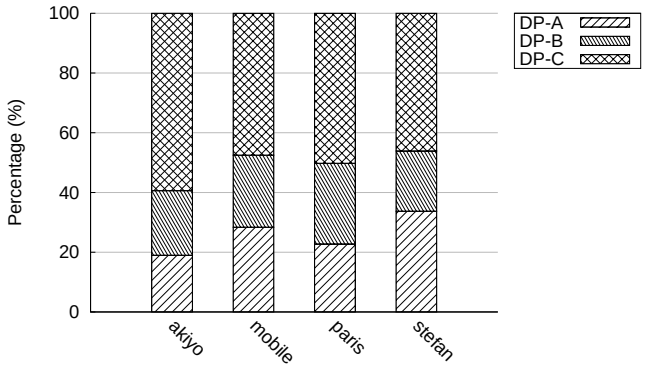

Figure 4. Percentage of data for partitions A, B and C in a variety of sequences with an intra-refresh line.

When coding a macroblock, inter- and intra-prediction modes are compared in terms of rate and distortion (RD) performance, selecting the prediction which achieves the lowest RD cost. If the encoder cannot find a suitable inter prediction (e.g. in a scene change or when a new object appears) then that macroblock is intra coded and its residual is written to DP-B. This is an implementation dependent decision as only the decoder is defined by the standard. In Figure 4, an intra-refresh MB line has been included. The growth in the size of DP-B is the main feature of this Figure. This is due to the fact that DP-B now includes naturally encoded MBs plus all forced intra-coded MBs from the inserted intra-refresh line. Figure 5, shows the resulting packet size distribution for the *Paris* video sequence with the same characteristics as employed in our evaluation of the proposed scheme. A 1 kB packet size constraint was imposed, representing a typical maximum transport unit size. Though the sizes of packets appear reasonably well distributed, as Figure 6 shows, the larger packets dominate the data transported.

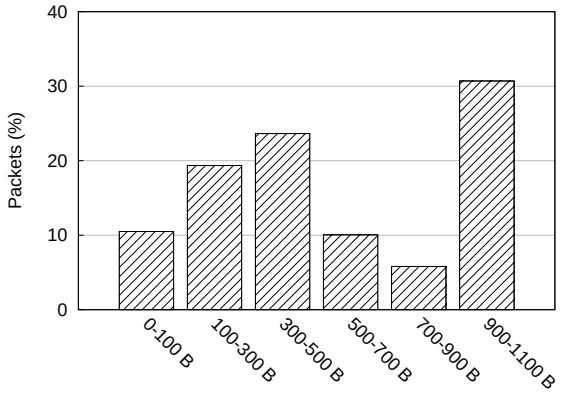

Figure 5. Packet size distribution when using data partitioning and a packet size limit of 1 kB for *Paris*.

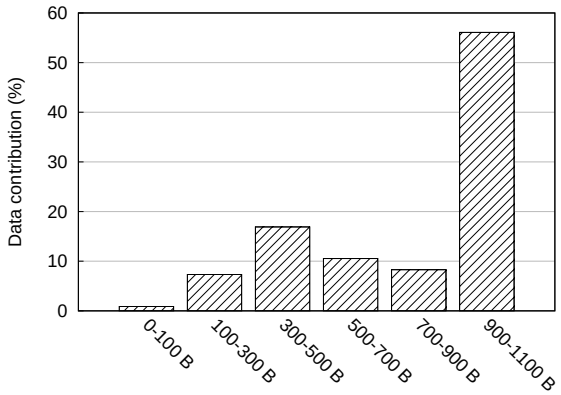

Figure 6. Stream data contribution for packet size ranges when using data partitioning and a packet size limit of 1 kB for *Paris*.

In this paper, the intra-refresh rate is dependent on the contribution of an intra-refresh MB line. It is also possible to decide upon the intra-refresh MB contribution depending on the likely distortion that would result at that rate. Distortion consists of two components: the distortion arising from source coding, D_s, and the distortion arising from channel errors harming the decoding of the received data, D_c. In (He et al., 2002) these distortion components are modeled for each frame as:

$$D_s = D_s(in) + \beta(1 - \lambda + \lambda\beta).[D_s(ia) - D_s(in)] \quad (1)$$

$$D_c = [(1 - \beta)(1 - p)b + p].D_c(n - 1) + pa.F_d(n, n - 1) \quad (2)$$

where $D_s(in)$ is the distortion if all MBs were to be inter-coded, $D_s(ia)$ is the distortion if all MBs were to be intra-coded, β is the intra-coding rate, λ is a source content factor, p is the probability of channel loss, a and b are codec dependent constants, and $F_d(n,n-1)$ is the mean-square error between frames n, and $n-1$. Unfortunately, there appears to be no closed form solution to minimizing $D = D_s + D_c$, according to a source rate R_s, and various constants are video sequence dependent. It is possible to find a closed-form solution for the mean value of D_c (He et al., 2002) if it is assumed that the channel loss probability is stationary over time. Unfortunately, this is a dubious assumption for wireless channel's affected by fast fading.

IEEE 802.11e EDCA and Access Category Mapping

IEEE 802.11e Enhanced Distributed Channel Access (EDCA) adds quality-of-service (QoS) support to legacy IEEE 802.11 wireless networks by introducing four Access Categories (ACs), i.e. AC0, AC1, AC2, and AC3 for background (BK), best-effort (BE), Video (VI) and Voice (VO) traffic respectively in order of increasing priority. Each AC has different Distributed Coordination Function (DCF) parameters for the Carrier Sense Multiple Access/Collision Avoidance (CSMA/CA) back-off mechanism. The parameters include contention window minimum (CWmin) and maximum (CWmax) sizes, arbitrary inter-frame space (AIFS) and transmission opportunity limit (TXOPLimit).

Figure 7 represents a practical implementation of the proposed prioritization scheme in which video packets are selectively mapped to IEEE 802.11e's EDCA queues. In this scheme, DP-A and DP-C packets are mapped to AC2 as this is the default AC for video traffic while DP-B packets are mapped to the lower priority AC1. The effect is to delay access to the channel for numerically lower indexed AC queues, thus increasing the probability that packets from these queues will be dropped through buffer overflow as additional packets arrive. This mapping scheme is further examined in the next Section.

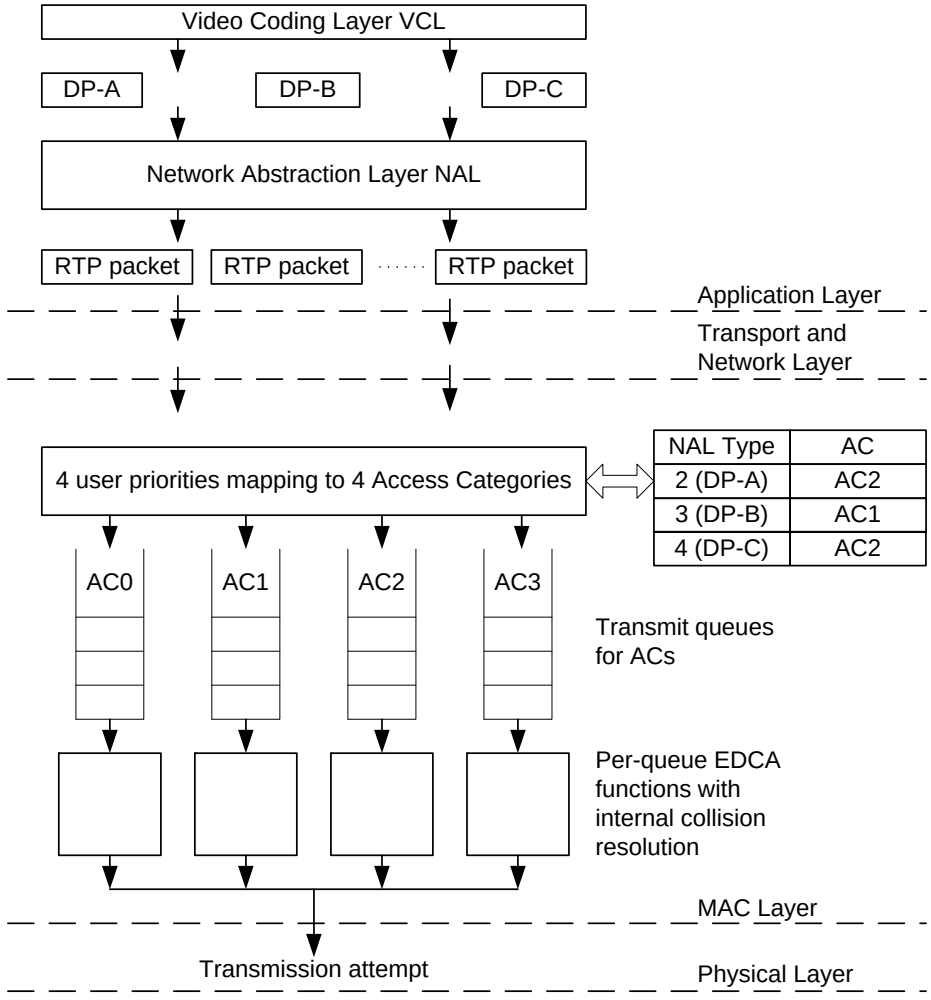

Figure 7. Proposed IEEE 802.11e access category mapping for the data-partitioned video.

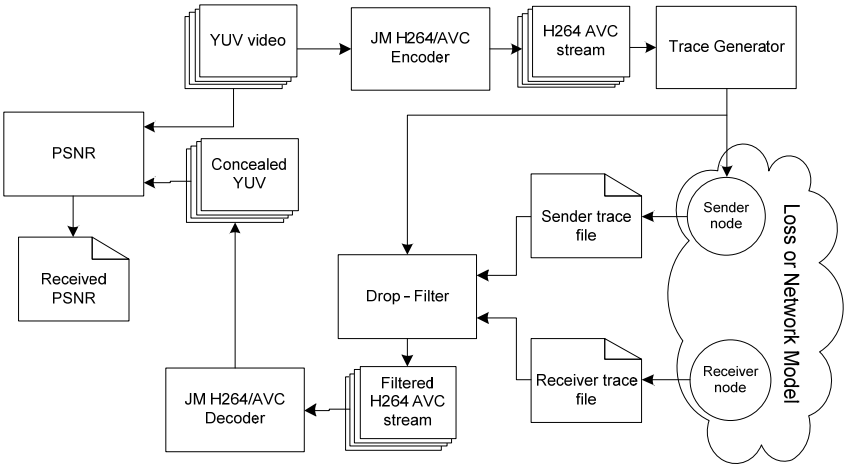

Figure 8. Video assessment framework.

EVALUATION

Video Assessment Framework

Figure 8 shows the evaluation framework for assessing the impact on video quality. The uncompressed test sequences are encoded according to the previously described settings to generate H.264/AVC compressed streams. After compression, these streams were parsed to produce trace files containing the size and transmission schedule for each packet. These traces were fed to either a loss model for random drop tests or to an ns-2 simulated congestion scenario. Comparing the sent trace file with the receiver's trace of packets received, the dropped packets were found. The dropped packets were removed from the original compressed stream to generate the damaged received stream. The received stream was then decoded using the H.264/AVC decoder with motion-copy error concealment (Wu & Boyce, 2006) enabled to reconstruct the uncompressed video and regenerate the lost slices. The resulting luminance Peak Signal-to-Noise Ratio (PSNR) of the received video was then obtained by comparing the original with the decoded uncompressed video. A total of 2000 runs were used for each set of simulations and the standard absolute PSNR deviations were calculated over intervals of 0.5 % video data drop. When packet sizes are widely spread as in Figure 5, a high packet drop rate might not represent a corresponding high data drop rate. Therefore, to make the results more accurate, the percentage of video data drop has been used instead of the packet drop rate. In the next section, a packet loss model has been used to introduce uniformly distributed packet drops.

Results for uniform packet drops

In order to evaluate the performance of the proposed scheme, four CIF test sequences (*Akiyo*, *Paris*, *Mobile* and *Stefan*), with 299 frames, were coded using the H.264/AVC reference software JM16.1 (JVT, 2010) at 30 frame/s. An IPPP coding structure and a target bitrate of 1 Mbps was used. Real-Time Protocol (RTP) packetization (Perkins, 2003), data partitioning and one intra-refresh MB line per frame were also enabled.

Simple analysis of the NAL headers allows an easy identification of the partition type of each packet. A percentage of video packets were dropped according to the following criteria. The

packets were simply separated into three different categories according to the partition type (A, B or C) and a number were randomly selected to be dropped up to a desired percentage.

Figure 9 gives the video quality obtained after: (i) dropping packets from DP-A packets only (drop DP-A); (ii) dropping packets from DP-B packets only (drop DP-B); (iii) dropping packets from DP-C packets only (drop DP-C); and (iv) dropping data randomly from any partition packets (drop any). Figure 9 shows that dropping packets from DP-A introduces a significant PSNR penalty that can be greater than 3 dB when compared with dropping randomly from any partition type. Contrary to the previous case, dropping packets exclusively from DP-B results in a quality gain of about 3 dB over dropping randomly. Finally, dropping only from DP-C produces results close to dropping randomly from any partition type. This is because DP-C is the dominant partition and when dropping randomly, it is more likely that packets belonging to DP-C will be dropped.

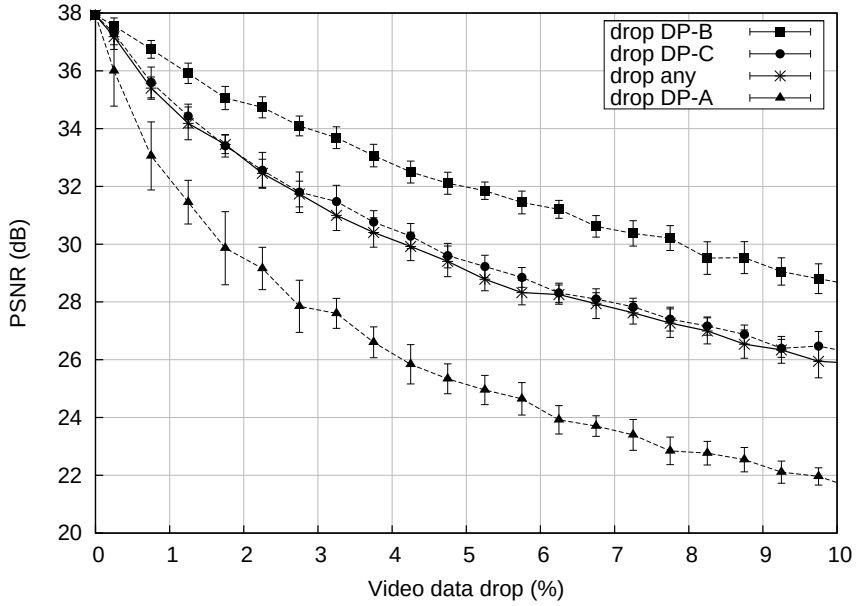

Figure 9. PSNR vs. percentage video data drop for *Paris*, with absolute standard error bars included.

Figures 3 and 4 showed that an intra-refresh MB line can contribute to a significant percentage of the video data as is noticeable from the increased percentage of DP-B data occurring when an intra- refresh MB line is introduced. All the same, an intra-refresh line only represents a single row of MBs per frame. Although a significant portion of the whole bitrate is expended encoding intra MB slices, only a small area of the image is represented by such a high number of bits. Therefore, the penalty in picture quality is low because error concealment is more efficient when small image areas are lost. The above procedures were repeated for many other sequences and the results are shown in Table 2. The results show the quality gain when dropping DP-B packets over dropping randomly (drop any) for different data drop percentages. The overall conclusion is that when intra refresh is used, DP-B packets are less important than DP-C packets.

Table 2. PSNR gain when dropping DP-B packets over dropping randomly for a range of different sequences.

% Video data drop	PSNR gain (dB)			
	Akiyo	Mobile	Paris	Stefan
0.25	0.6	0.4	0.1	0.4
0.75	3.2	1.4	0.3	1.3
1.25	3.2	1.9	0.6	2.2
1.75	5.3	2.4	0.8	2.7
2.25	3.9	2.5	1.2	3.5
2.75	4.9	3.2	1.2	3.4
3.25	5.4	3.2	1.4	3.8
3.75	4.9	2.8	1.5	4.0
4.25	5.6	3.7	1.8	4.3
4.75	5.6	3.2	2.1	4.1
5.25	5.1	3.1	2.3	4.4
5.75	4.7	3.3	2.5	4.6
6.25	5.2	3.3	2.4	4.7
6.75	4.6	3.3	2.8	4.8
7.25	5.1	2.9	3.1	5.0
7.75	4.5	3.2	3.1	5.2
8.25	5.3	3.1	3.0	4.9
8.75	4.0	2.8	3.1	5.5
9.25	4.1	2.6	2.9	5.0
9.75	4.1	2.6	3.1	5.2

Effect of congestion in a wireless network

In this Section, we simulate the behavior of the scheme in the presence of congestion within a multi-hop wireless network in which one of the sources is streaming video. Two scenarios have been tested, one adequate for indoor environments and the second for the outdoors. Three sets of tests were performed. In the proposed scheme (*prop*) tests, the video data packets belonging to DP-A and DP-C were assigned to AC2 while those belonging to DP-B were assigned to AC1. For the alternative mapping scheme (*alter*), DP-A and DP-B packets were assigned to AC2 while DP-C packets were assigned to AC1. For the last set of tests (*deflt*), video stream packets were simply assigned to AC2, the default IEEE 802.11e video access category.

The same video-encoding configurations used for the uniform drops were employed in the following tests. We employed the IEEE 802.11e EDCA Media Access Control (MAC) simulation model developed by the Technical University of Berlin, 2003 for the well-known ns-2 simulator. The EDCA parameter values in Table 3 for the IEEE 802.11b radio were employed. The IEEE 802.11b physical layer was modeled with a data-rate of 11 Mbps and a basic rate of 1 Mbps. Other common simulation parameters are shown in Table 4.

Table 3. IEEE 802.11e MAC parameter values for the IEEE 802.11b radio

Access Category	*AIFSN*	*CWmin*	*CWmax*	*TXOPLimit (ms)*
AC0 (Background)	7	31	1023	0
AC1 (Best Effort)	3	31	1023	0
AC2 (Video: VI)	2	15	31	6.016
AC3 (Voice: VO)	2	7	15	3.264

Table 4. Common simulation parameters.

Parameter	Value
Frequency band	2.4 GHz
Data rate	11 Mbps
Interface queue	Priority queue
Interface queue length	60
Transmit power	0.28 W
Antenna type	Omni-directional
Antenna gain	1
Antenna length	1 m
Antenna height	1.5 m

Indoor Scenario

This scenario was set up to simulate an indoors (factory, obstructed) environment. The static scenario is shown in Figure 10 which consists of a line of four nodes 25 m apart in which the two intermediate nodes can be considered as repeaters. In these simulations, we used the shadowing propagation model (Rappaport, 2002) which is widely adopted for cellular radio systems. For this model, the mean large-scale received power is:

$$\overline{P_r}(d)[\text{dB}] = 10\,log\,P_r(d_0) - 10n\,log\left(\frac{d}{d_0}\right) \tag{3}$$

where d_0 is the close-in reference distance, d is the receiver transmitter separation, and n is the path loss exponent. The value of $P_r(d_0)$ is usually calculated using the free space model for a distance d_0 from the transmitter:

$$P_r(d) = P_t \frac{\lambda^2}{(4\pi)^2 d^2} G_t G_r \tag{4}$$

where P_t is the transmitter power, λ is the wavelength and G_t and G_r are the gains of the transmitter and receiver antennas respectively.

To model shadowing, an additive zero-mean Gaussian factor with standard deviation σ[dB] is applied to give the instantaneous received signal power:

$$P_r(d)[\text{dB}] = \overline{P_r}(d) + X_\sigma \tag{5}$$

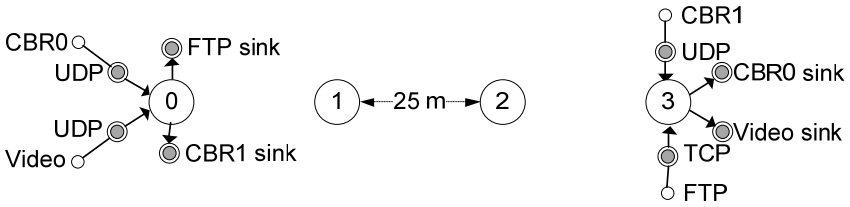

Figure 10. Network topology used for the indoor simulations.

Table 5. Traffic in the scenario of Figure 10.

Traffic type	*Source node*	*Destination node*	*IEEE 802.11e AC*	*Transport protocol*	*Datarate kbps*
CBR0	0	3	3	UDP	0 – 160
Video	0	3	1 and 2	UDP	1000
CBR1	3	0	1	UDP	128
FTP	3	0	0	TCP	Varied

In the simulations with the shadowing model, n =4, d_o = 1 m, and σ = 6, which match the indoor scenario according to in-the-field measurements (Rappaport, 2002).

Table 5 shows the traffic sources in this scenario and their associated nodes and IEEE 802.11e access categories.

Figure 11 shows the video quality versus percentage video data drop. It is clear that applying the proposed mapping scheme (*prop*) will give higher PSNR (up to 2 dB) values than when the video stream is entirely assigned to AC2 (*deflt*). It can also be seen that giving priority to DP-B over DP-C (*alter*) results in a smaller PSNR gain (up to 1 dB) when compared with sending all partition types over AC2. Figure 12 shows the end-to-end delay. As expected, the penalty of the scheme is that some video packets are assigned to the lower priority AC1 queue. As a result, their queuing time is increased. The increase is greater when there is more congestion, which is also when there are more packet drops.

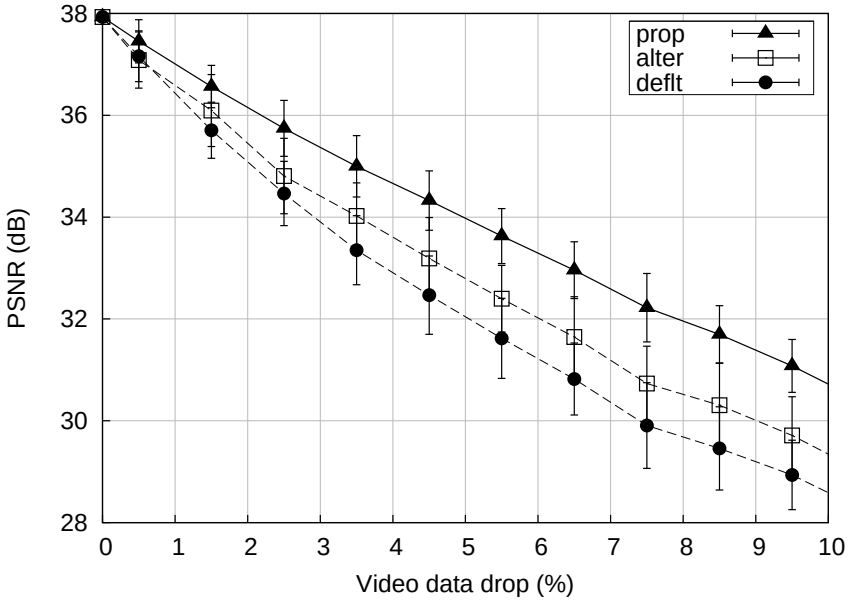

Figure 11. PSNR vs. percentage video data drop for *Paris*, with absolute standard error bars included.

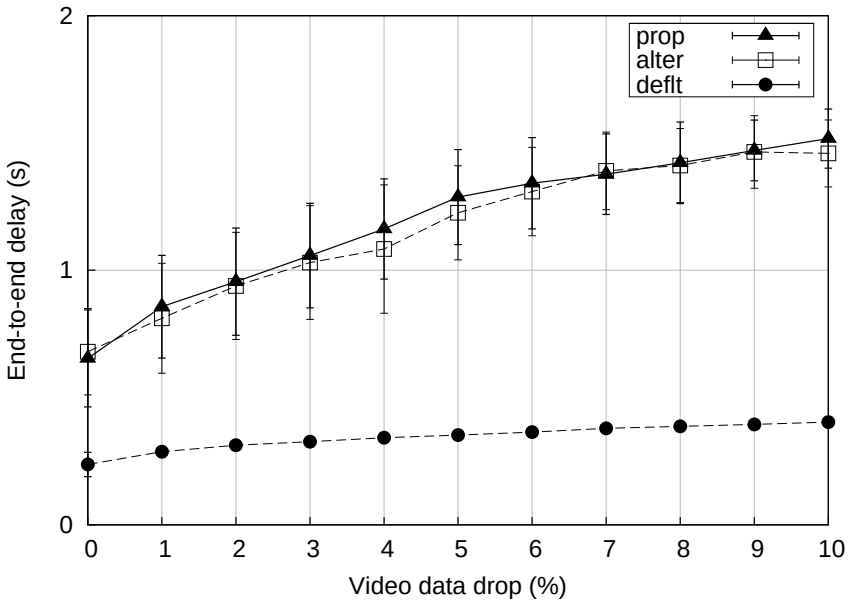

Figure 12. Mean end-to-end delay versus percentage video data drop for *Paris*, with absolute standard error bars included.

Outdoor scenario

For this scenario, which is shown in Figure 13, nodes were static with all adjacent ones 200 m apart. The Ad-hoc On-Demand Distance Vector (AODV) (Perkins et al., 2003) routing protocol was now deployed with control packets carried at higher-priority AC3. The two-ray ground reflection propagation model (Rappaport, 2002) was used in this scenario which better fits line-of-sight outdoor environments. For this model, the received power at a distance d from the transmitter is given by

$$P_r(d) = P_t \frac{h_t^2 h_r^2}{d^4} G_t G_r \qquad (6)$$

where h_t and h_r are the heights of the transmitter and receiver antennas respectively.

The contributing traffic sources for this scenario and their mapping to IEEE 802.11e ACs are shown in Table 6.

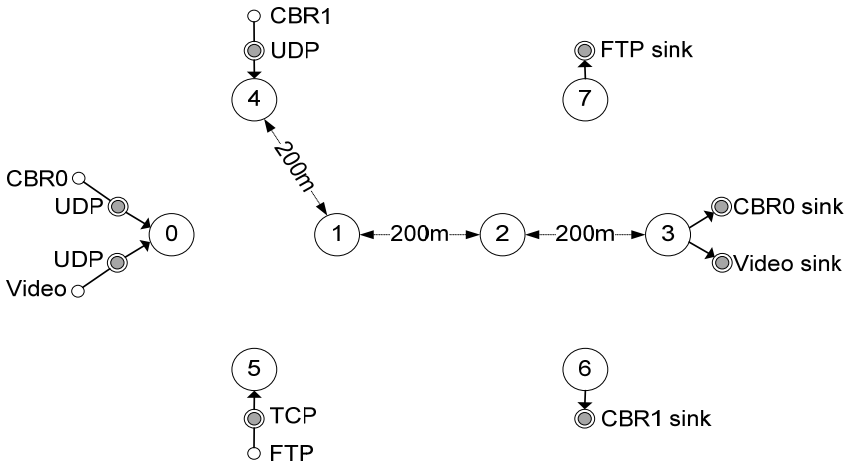

Figure 13. Network topology used for the outdoor simulations.

Table 6. Traffic in scenario of Figure 13.

Traffic	*Source node*	*Destination node*	*AC*	*Transport*	*Value kbps*
CBR0	0	3	3	UDP	48-224
Video	0	3	1 and 2	UDP	1000
CBR1	4	6	1	UDP	128
FTP	5	7	0	TCP	Varied

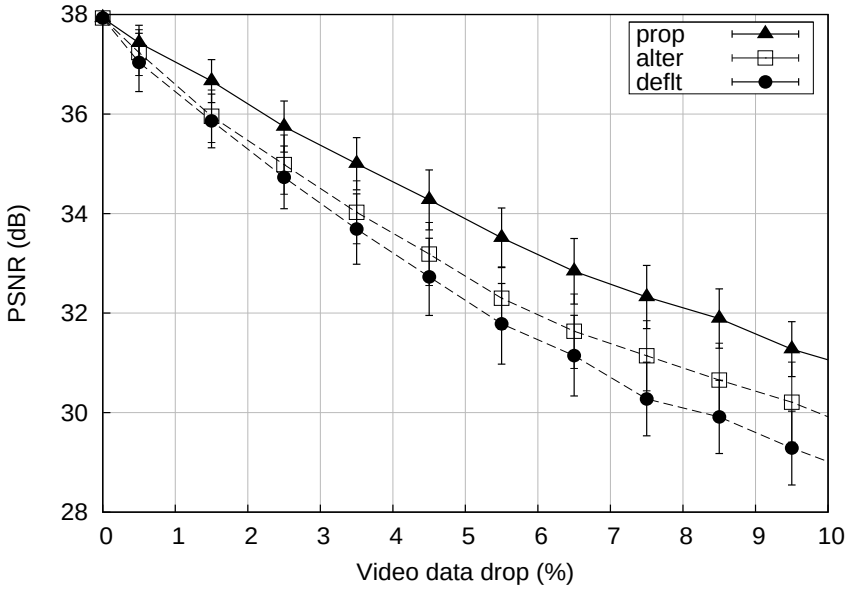

Figure 14. PSNR vs. percentage video data drop for *Paris*, with absolute standard error bars included.

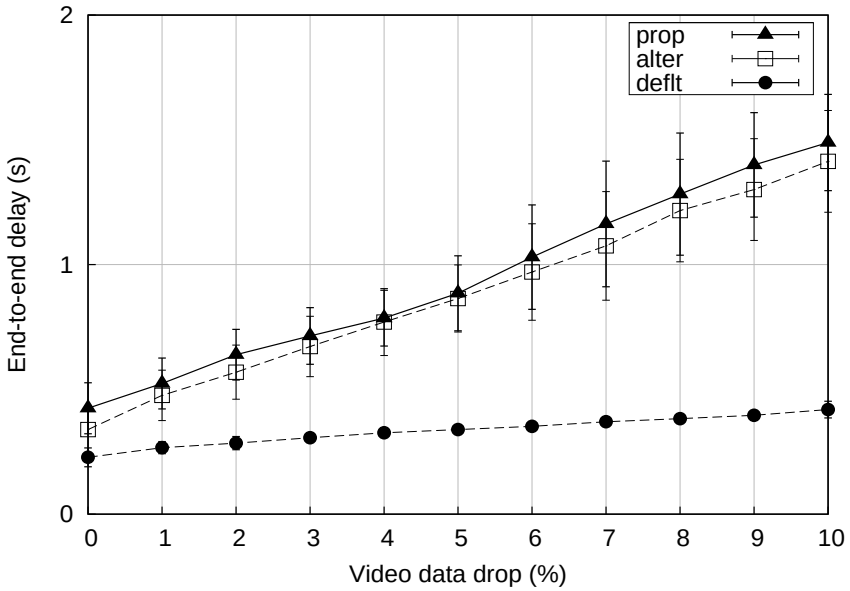

Figure 15. Mean end-to-end delay versus percentage video data drop for *Paris*, with absolute standard error bars included.

Figure 14 shows the video quality versus percentage video data drop. Again, the proposed scheme overcomes both other schemes. The overhead of assigning some video packets to AC1 is an increased end-to-end delay as shown in Figure 15.

We also tested the schemes for the quality gain over assignment to AC2 for the same set of video sequences coded for the uniform drop tests. In Table 7, the comparison is between the proposed scheme and the alternative scheme for data-partitioning prioritization. As will be easily observed, in almost all cases both schemes result in better video quality than sending video over AC2 alone. Moreover, the proposed scheme is always superior to the alternative scheme.

Table 7. PSNR gain from the proposed scheme (*prop*) and the alternative scheme (*alter*) over the default IEEE 802.11e video assignment scheme (*deflt*) across a range of different sequences.

% Video data drop	PSNR gain in dB Proposed scheme (*prop*): DP-A & DP-C sent over AC2 , DP-B sent over AC1 Alternative scheme (*alter*): DP-A & DP-B sent over AC2, DP-C sent over AC1							
	Akiyo		*Mobile*		*Paris*		*Stefan*	
	prop	*alter*	*prop*	*alter*	*prop*	*alter*	*prop*	*alter*
0	0.00	0.00	0.00	0.00	0.00	0.00	0.00	0.00
0.5	0.35	-0.05	0.64	0.59	0.39	0.20	0.35	-0.09
1.5	0.73	0.22	1.47	1.24	0.80	0.09	0.77	-0.31
2.5	1.37	0.69	1.53	1.31	1.02	0.26	0.98	-0.55
3.5	1.46	0.71	1.24	1.46	1.31	0.34	0.83	-0.09
4.5	1.39	0.49	1.35	1.14	1.55	0.46	0.62	0.09
5.5	1.09	0.89	1.93	1.58	1.73	0.51	0.54	0.32
6.5	1.49	1.27	2.21	1.65	1.70	0.49	1.10	0.50
7.5	0.82	0.68	1.77	1.56	2.05	0.87	0.83	0.58
8.5	0.92	1.03	2.54	1.55	1.98	0.74	1.14	1.10
9.5	0.59	0.68	2.30	1.56	1.99	0.92	0.50	1.15

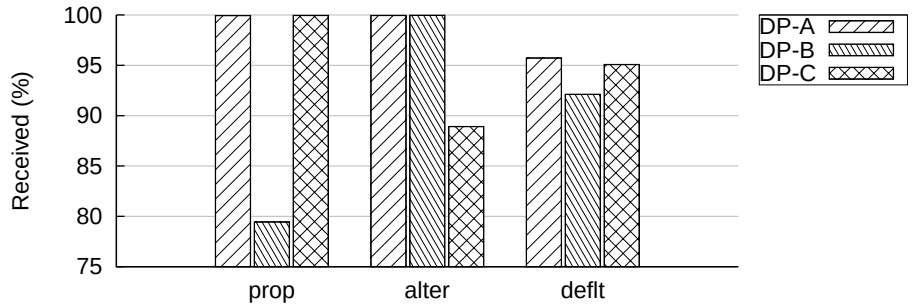

Figure 16. Mean received percentages of data partitions A, B and C for 150 runs at 5% video data drop rate for the three tested schemes for *Paris*.

Figure 16 shows the mean received percentages of data partitions A, B and C at 5% video data drop for the three tested schemes. The mean is calculated over 150 runs for the *Paris* test sequence. The figure shows that the proposed scheme is the best to protect data partitions A and C while the sending video over AC2 expose the most important data partition A to a considerable loss and hence the bad assessed video quality. The alternative scheme protects well DP-A and DP-B while there is a considerable loss in DP-C. The fact that the video quality assessed at this point show higher values for the proposed scheme demonstrates that DP-C packets should be given priority over that of DP-B. Tests for the scenario of Figure 13 were repeated using the shadowing propagation model and results again showed the usefulness of the proposed scheme. However, as the results were close to those previously given, they are not reported herein.

CONCLUSION

In this paper, the contrasting goals of congestion resilience and transmission error resilience have been highlighted. Because the presence of intra-refresh MBs assists the process of error resilience it is easy to assume that partition-B data should be given higher priority access to a WLAN in preference to the transform coefficients collected into partition-C packets. When the size of the B-partition is increased due to the presence of intra-refresh MBs then this is not so. In fact, in all the results in this paper, dropping partition-B data first was preferable. However, including an intra-refresh MB line is a normal procedure to avoid the presence, when periodic I-frames are used, of sudden increases in bandwidth, which is a significant problem for bandwidth-limited wireless networks. The scheme in this paper proposes assigning low priority to DP-B packets when intra-refresh lines are used. Applying the proposed scheme, for congested networks, a PSNR gain of up to 2 dB is obtained in comparison to the case when no prioritization is used at all. Compared with other data partition prioritization schemes, the proposed scheme is still able to achieve up to 1 dB PSNR gain. The value of the scheme has been confirmed for a variety of channel models and conditions in indoor and outdoor WLANs. Therefore, this paper has shown that previous schemes, mainly intended for prioritized transmission of data-partitioned video should also take into account the presence of intra refresh in the stream. Future work will consider whether the scheme should distinguish between inserted intra-refresh line MBs and naturally encoded intra MBs.

REFERENCES

Afzal, J., Stockhammer, T., Gasiba, T. & Xu, W. (2006). Video streaming over MBMS: A system design approach. *Journal of Multimedia, 1(5)*, 25-35.

Ali, I., Moiron, S., Fleury, M., & Ghanbari, M. (2010). Congestion resiliency of data partitioned H.264/AVC video over wireless networks. In *7th International ICST Mobile Multimedia communications*.

Barma, B., Ghandi, M.M., Jones, E.V., & Ghanbari, M. (2005). Prioritized transmission of data-partitioned H.264 video with hierarchical modulation. *IEEE Signal Processing Letters, 12(8)*, 577-580.

Bernardini, R., Durigon, M., Rinaldo, R., Zontone, P., & Vitali, A. (2007). Real-time multiple description video streaming over QoS-based wireless networks. In *IEEE International Conference on Image Processing* (pp. 245-248).

Cranley, N., Debnath, T., & Davis, M. (2007). An experimental investigation of parallel multimedia streams over IEEE 802.11e WLAN networks using TXOP. In *IEEE International Conference on Communications* (pp. 1740-1746).

Dhondt, Y., Mys, S., Vermeirsch, K., & Van de Walle, R. (2007). Constrained Inter Prediction: Removing Dependencies between Different Data Partitions. In *Proceedings of Advanced Concepts for Intelligent Visual Systems* (pp. 720-731).

Haywood, R., Mukherjee, S. & Peng, X.-H. (2009). Investigation of H.264 video streaming over an IEEE 802.11e EDCA wireless testbed. In *IEEE International Conference on Communications*, (pp. 1-5).

He, J., Cai, J. & Wen Chen, C. (2002). Joint source channel rate-distortion analysis for adaptive mode selection and rate control in wireless video coding. (2002). *IEEE Transactions on Circuits and Systems for Video Technology, 12(6)*, 511-523.

IEEE. (2005). Wireless LAN Medium Access Control and Physical Layer Specifications Amendment 8: Medium Access Quality of Service Enhancements. *IEEE Std 802.11e-2005*.

JVT, (2010). Reference Software Version JM16.1. [Online] http://iphome.hhi.de/suehring/tml/download/old jm/jm16.1.zip.

Ksentini, A., Naimi, M., & Guroui, A. (2006). Toward an improvement of H.264 video transmission over IEEE 802.11e through a cross-layer architecture. *IEEE Communications Magazine, 44(1)*, 107-114.

Liang, Y.J., El-Maleh, K. & Manjunath, S. (2006). Upfront intra-refresh decision for low-complexity wireless video telephony. In *IEEE International Symposium on Circuits and Systems*.

Liu, L., Ye, X.-J., Zhang, S.-Y., & Zhang, Y. (2005). H.264/AVC error resilience tools suitable for 3G mobile video services. *Journal of Zhejiang University SCIENCE, 6(4)*, 1-46.

Perkins, C. (2003). RTP: *Audio and Video for the Internet*. Indianapolis, IN: Addison-Wesley Professional.

Perkins, C., Belding-Royer, E.; Das, S. (2003). Ad hoc On-Demand Distance Vector (AODV) routing. Internet Engineering Task Force, RFC 3561.

Rappaport, T.S. (2002). *Wireless communications: Principles and practice*. Upper Saddle River, NJ: Prentice Hall.

Schreier, R.M. & Rothermel, A. (2006). Motion adaptive intra refresh for the H.264 video coding standard. *IEEE Transactions on Consumer Electronics, 52(1)*, 249-253.

Stockhammer, T., Hannuksela, M.M. & Wiegand, T. (2003). H.264/AVC in wireless environments. *IEEE Transactions on Circuits and Systems for Video Technology, 13(7)*, 657-673.

Stockhammer, T. & Hannuksela, M.M. (2005). H.264/AVC video for wireless transmission. *IEEE Wireless Communications. 12(4),* 6-13.

Technical University of Berlin, (2003). An IEEE 802.11e EDCA and CFB Simulation Model for ns-2. [online] http://www.tkn.tu-berlin.de/research/

Tran, T.D., Liu, L.K., & Westering, P.H. (1998). Low-delay MPEG-2 video coding. In SPIE - International Society of Optical Engineers (USA), 3309, (pp. 510-516).

Wenger, S. (2003). H.264/AVC over IP. *IEEE Transactions on Circuits and Systems for Video Technology, 13(7)*, 645-656.

Wiegand, T., Sullivan, G.J., Bjontegaard, G., & Luthra, A. (2003). Overview of the H.264/AVC video coding standard. *IEEE Transactions on Circuits and Systems for Video Technology, 13(7)*, 560-576.

Wu, Z. and Boyce, J.M. (2006). An error concealment scheme for entire frame losses based on H.264/AVC. In *IEEE International Symposium on Circuits and Systems* (pp. 4463-4466).